Microstrip to Ridge Gap Waveguide Transition for 28 GHz Steerable Slot Array Antennas

Alireza Bagheri*†, Hanna Karlsson*, Carlo Bencivenni*, Abolfazl Haddadi*,
Thomas Emanuelsson*‡, Andrés Alayón Glazunov†‡
*Gapwaves AB, Gothenburg, Sweden
†University of Twente, Enschede, Netherlands
‡Chalmers University of Technology, Gothenburg, Sweden

***Abstract*—In this paper three types of contactless vertical transitions from microstrip to double ridge waveguide are presented. The designs are compact in size and robust, with improved isolation by employing a pin structure, making them ideal for 5G mmWave phased arrays. All transitions cover the $26.5-29.5$ GHz band, their dimensions are less than half a wavelength in pitch and have insertion losses less than 0.6 dB. The three designs apply different matching strategies and offer a trade-off between bandwidth and PCB areas. Finally, the behavior within an array configuration is analyzed.**

I. Introduction

It is well-known that the gap waveguide is an advantageous wave guiding solution for mmWave frequency bands. Indeed, it provides attractive characteristics such as low-loss, wide bandwidth and ease of manufacture [1]. This technology is based on the concept of two parallel PEC and PMC plates, which when placed less than a quarter of wavelength apart, prevents wave propagation in undesired directions while allowing wave propagation along a desired path. A guiding structure is then obtained when the appropriate geometry is inserted, e.g., in the form of the groove, the microstrip and the inverted microstrip gap waveguides [2]. Similarly to classical waveguides, a ridged gap waveguide is obtained by placing a metal strip in a hollow cavity. This configuration supports a quasi-TEM propagation mode in a compact and low-loss fashion. In order to implement the PMC boundary, a bed of periodically arranged pins is typically used as an artificial magnetic conductor (AMC). In practice, the contactless nature of the gap waveguides helps for mass-producible antenna solutions, especially at microwave and mmWave frequencies [3]–[5].

However, all microwave technologies must offer good integration with PCB technology as the carrier of most, if not all, active components. It is thus important that such transitions offer good performance, robustness and simple integration. This is especially true in phased arrays for 5G applications, where the large number of densely packed antenna elements create issues of spacing and isolation [6], [7]. The three types of transitions presented in this paper target specifically this scenario and has thus been tested in an array configuration similar to previously published arrays [8], [9].

In the past years, a large number of microstrip to gap waveguide transitions have been designed. A horizontal contactless transition is presented in [10], but the one wavelength width makes it unsuitable for phased arrays. This issue is solved in [11] which is a horizontal, compact and contactless transition. However, verticals transition are the only practical solution for phased arrays as they leave the space below the antenna available for PCB routing and active components. Ultra-wideband transitions have also been proposed in [12], [13], but the need for galvanic contact between waveguide and microstrip make them sensitive to assembly [14]. Double- and single-ridge gap waveguides allow to design narrow waveguide-based radiating elements to be used in phased arrays with wide steering ranges. The proposed transitions can be used for gap waveguide-based arrays which has been investigated to be a promising solutions for upcoming 5G applications [5].

In this paper, three types of contactless vertical transitions with application in antenna arrays based on gap waveguide technology are proposed. Section II describes the design of transitions, Section III considers the integration with an antenna array with center-fed elements. Section IV provides the conclusions.

II. Transitions Design

The structure of the transitions is shown in Fig. 1. All three transitions consist of a PCB with a rectangular patch coupled to a double-ridge waveguide surrounded by a pin structure. The double-ridge waveguide has dimensions 4.25×2.1 mm with a ridge height of 1.4125 mm and a ridge width of 1.4 mm. The double-ridge is extended towards the PCB on each side of the waveguide opening to ensure sufficient coupling between the transition patch and the waveguide. The pin structure is designed to have a stopband in the desired frequency range, as to increase isolation between adjacent antenna columns, decrease leakage from microstrip patch, and consequently improving signal transmission level to double-ridge waveguide. The role of pin structure is very essential and the transitions do not work without them. The pin dimensions are 2.7×1.58 mm with a pin period of 2.8 mm. A 10 mils Rogers RO4350B-substrate with a relative dielectric constant of $\varepsilon_r = 3.66$ is used for the PCB, with a copper thickness of 0.035 mm and a microstrip width of 0.5 mm. The specific transition type configuration is explained below:

- Type 1 transition has a matching stub in series with the transition patch as shown in Fig. 1a. Both the size of the

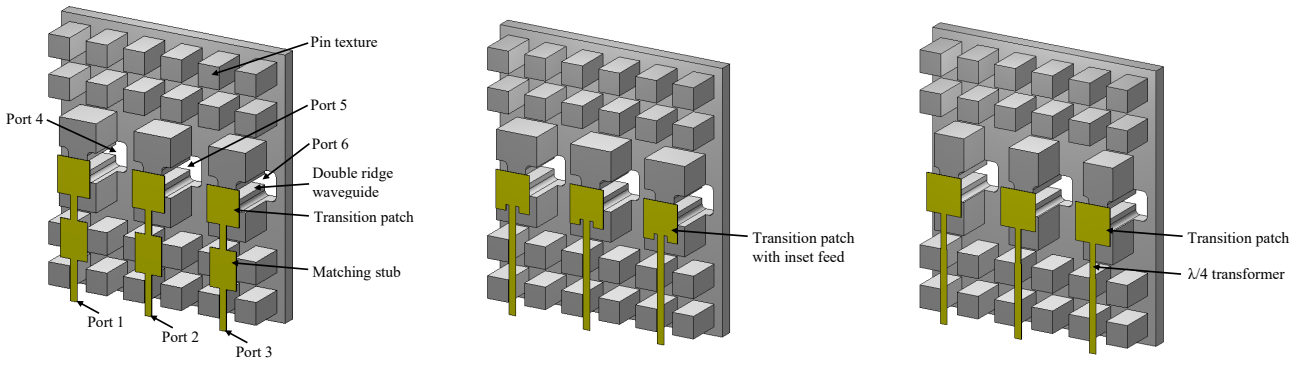

(a) Type 1 (b) Type 2 (c) Type 3

Fig. 1. The structure of three microstrip to double ridge waveguide transitions. In these figures, substrate and ground layer of microstrip lines are not shown.

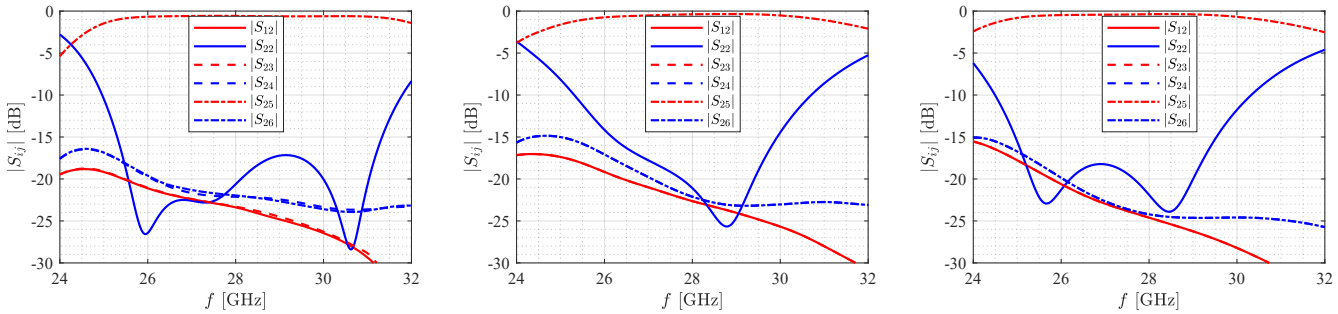

(a) Type 1 (b) Type 2 (c) Type 3

Fig. 2. Scattering parameters of each transition.

TABLE I
COMPARISON OF TRANSITIONS PERFORMANCES.

Transition	Bandwidth [GHz]		Max. insertion loss [dB] in 26.5 − 29.5 GHz	Advantage	Disadvantage
	$\lvert S_{22}\rvert < -15$ dB	$\lvert S_{22}\rvert < -10$ dB			
Type 1	6 (21.3%)	6.8 (24%)	0.62	Wideband	Not Compact
Type 2	3.7 (13.3%)	5.4 (19.2%)	0.6	Compact on PCB	Narrowband
Type 3	4.6 (16.8%)	5.8 (21.2%)	0.49	Relatively wideband	-

stub and the distance from the patch is tuned to achieve optimal performance. The patch and stub dimensions are 2.42×2.6 and 2×2.73 mm^2, respectively and have 1.7 mm distance.

- Type 2 transition is shown in Fig. 1b. It uses an inset of the feed into the patch. This gives a more compact design compared to the type 1 transition. Patch dimensions are 2.54×2.73 mm^2 and inset gap and length are 0.42 and 0.24 mm, respectively.
- Fig. 1c shows type 3 transition. It uses a quarter-wave transformer to transform the impedance of the microstrip to that of the transition patch. The patch and transformer dimensions are 2.6×2.68 and 0.43×2.44 mm^2.

The transition patch is optimized individually for each transition type regarding its length, width and center point offset relative the center point of the waveguide.

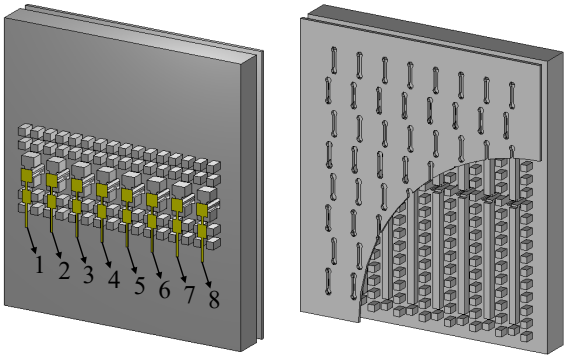

Fig. 3. Integration of transition type 1 with a 5G antenna array based on gap waveguide technology [9]. A part of slot layer is cut for viewing purposes. The number of port for each microstrip line is shown in left side picture.

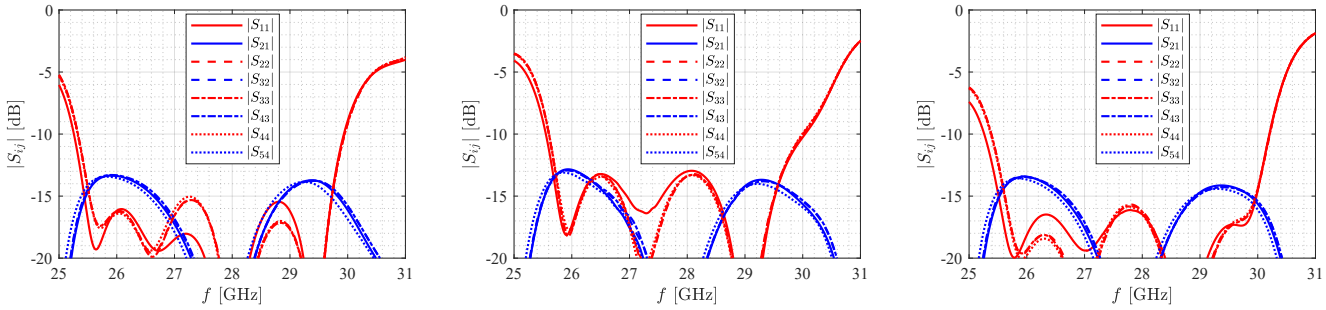

(a) Type 1 (b) Type 2 (c) Type 3

Fig. 4. Reflection coefficient and coupling coefficients with neighbor ports in the array, when the transitions are used to excite the antenna.

The software Computer Simulation Technology (CST) was used for simulating and optimizing the three transition types. The scattering parameters of each transition are shown in Fig. 2a- 2c, where the port numbering corresponds to Fig. 1. For transition type 1, the scattering parameters in Fig. 2a shows a wideband performance with a 15 dB return loss bandwidth of 21.3% while having an insertion loss of maximum 0.62 dB within the band of interest. The coupling to the adjacent transition columns is kept below -15 dB throughout the whole simulation range and is less than 20 dB for $26.5 - 29.5$ GHz. The scattering parameters for transition type 2 is shown in Fig. 2b displaying a 15 dB return loss bandwidth of 13.3% and an isolation towards neighboring columns higher than 17 dB between $26.5 - 29.5$ GHz. The maximum insertion loss within the frequency band is 0.6 dB for transition type 2. For type 3, the results are displayed in Fig. 2c and shows a 15 dB return loss bandwidth of 16.8% with a maximum insertion loss of 0.49 dB.

A summary of the performance of all three transition types is given in Table I, where advantages and disadvantages are also listed. Comparing the results shows that transition type 1 gives a wideband performance, while being less compact to other solutions. Type 2 is the most compact of the transitions but comes with the disadvantage of being less wideband compared to type 1 and 3.

III. Integration with 5G Antenna

To further study the performance of the proposed transitions, we consider the integration with a previously designed phased array based on gap waveguide technology [9]. Note that neither the antenna nor the transition has been tuned to each other, thus sub-optimal performance is expected. The front and back view of the complete antenna and type 1 transition assembly are shown in the left and right side of Fig. 3, respectively. The array is composed by 8 center-fed subarrays of 8 longitudinal and horizontally polarized slots. The horizontal spacing between columns is 5.6 mm ($0.52\lambda_0$ at 29.5 GHz).

Fig. 4 shows the embedded scattering parameters of the array ports, when the three types of transitions are used. Due to symmetry in the structure, simulation results for ports 5 to 8 are omitted. The antenna array integrated with every types of transitions has scattering parameters below -10 dB, without any retuning for the new transitions. The coupling coefficients for adjacent ports are better than -13 dB, with the non-contiguous being below -20 dB.

IV. Conclusion

Three types of microstrip-to-ridge-gap-waveguide are presented in this paper. Their characteristics, including return loss, insertion loss and isolation are discussed. Transitions are vertical, compact and contactless. They are designed for $26.5 - 29.5$ GHz, which all types show insertion loss less than 0.6 dB, return loss less than -15 dB and isolation better than 20 dB. These features make them ideal for 5G mmWave phased arrays based on gap waveguide technology. All transitions are designed for 28 GHz as the center frequency and their performance is evaluated when integrated with a previously designed antenna array.

Acknowledgment

This project has received funding from the European Union Horizon 2020 research and innovation program under the Marie Skłodowska-Curie grant agreement No. 766231 WAVECOMBE H2020-MSCA-ITN-2017.

References

[1] P.-S. Kildal, A. U. Zaman, E. Rajo-Iglesias, E. Alfonso, and A. Valero-Nogueira, "Design and experimental verification of ridge gap waveguide in bed of nails for parallel-plate mode suppression," *IET Microwaves, Antennas & Propagation*, vol. 5, no. 3, pp. 262–270, 2011.

[2] A. U. Zaman and P. S. Kildal, "Gap waveguides for mmwave antenna systems and electronic packaging," *chapter in Handbook of Antenna Technologies, Springer*, 2016.

[3] E. Alfonso, A. Haddadi, S. Carlsson, T. Emanuelsson, and J. Andren, "Developments towards the mass-production of high-gain gap-based planar antennas for radio links," in *12th European Conference on Antennas and Propagation (EuCAP 2018)*, pp. 1–4, April 2018.

[4] A. Vosoogh, A. Haddadi, A. U. Zaman, J. Yang, H. Zirath, and A. A. Kishk, "W-band low-profile monopulse slot array antenna based on gap waveguide corporate-feed network," *IEEE Transactions on Antennas and Propagation*, vol. 66, no. 12, pp. 6997–7009, 2018.

[5] C. Bencivenni, A. U. Zaman, A. Haddadi, and T. Emanuelsson, "Towards integrated active antennas for 5G mm-wave applications at gapwaves," in *2018 IEEE International Symposium on Antennas and Propagation & USNC/URSI National Radio Science Meeting*, pp. 415–416, IEEE, 2018.

[6] M. Khalily, R. Tafazolli, P. Xiao, and A. A. Kishk, "Broadband mm-wave microstrip array antenna with improved radiation characteristics for different 5G applications," *IEEE Transactions on Antennas and Propagation*, vol. 66, no. 9, pp. 4641–4647, 2018.

[7] P. A. Dzagbletey and Y.-B. Jung, "Stacked microstrip linear array for millimeter-wave 5G baseband communication," *IEEE Antennas and Wireless Propagation Letters*, vol. 17, no. 5, pp. 780–783, 2018.

[8] C. Bencivenni, M. Gustafsson, A. Haddadi, A. U. Zaman, and T. Emanuelsson, "5g mmwave beam steering antenna development and testing," in *2019 13th European Conference on Antennas and Propagation (EuCAP)*, pp. 1–4, IEEE, 2019.

[9] A. Bagheri, C. Bencivenni, and A. A. Glazunov, "mmwave array antenna based on gap waveguide technology for 5G applications," in *2019 International Conference on Electromagnetics in Advanced Applications (ICEAA)*, IEEE, 2019.

[10] B. Molaei and A. Khaleghi, "A novel wideband microstrip line to ridge gap waveguide transition using defected ground slot," *IEEE Microwave and Wireless Components Letters*, vol. 25, no. 2, pp. 91–93, 2015.

[11] A. A. Brazález, J. Flygare, J. Yang, V. Vassilev, M. Baquero-Escudero, and P.-S. Kildal, "Design of f-band transition from microstrip to ridge gap waveguide including monte carlo assembly tolerance analysis," *IEEE Transactions on Microwave Theory and Techniques*, vol. 64, no. 4, pp. 1245–1254, 2016.

[12] A. U. Zaman, T. Vukusic, M. Alexanderson, and P.-S. Kildal, "Design of a simple transition from microstrip to ridge gap waveguide suited for mmic and antenna integration," *IEEE Antennas and wireless propagation letters*, vol. 12, pp. 1558–1561, 2013.

[13] S. Peng, Y. Pu, W. Shao, X. Wang, and Y. Luo, "A broadband ridge gap waveguide to micro-strip transition using probe current coupling," in *2019 International Vacuum Electronics Conference (IVEC)*, pp. 1–2, IEEE, 2019.

[14] Z. Liu and D. Sun, "Transition from rectangular waveguide to empty substrate integrated gap waveguide," *Electronics Letters*, vol. 55, no. 11, pp. 654–656, 2019.